Double-stranded RNA promotes CTL-independent tumor cytolysis mediated by CD11b^{+}Ly6G^{+} intratumor myeloid cells through the TICAM-1 signaling pathway

Hiroaki Shime[1*], Misako Matsumoto[1], and Tsukasa Seya[1]

[1]Department of Microbiology and Immunology, Hokkaido University Graduate School of Medicine, Kita 15, Nishi 7, Kita-ku, Sapporo 060-8638, Japan.

*Corresponding author: Hiroaki Shime, Department of Microbiology and Immunology, Hokkaido University Graduate School of Medicine, Kita 15, Nishi 7, Kita-ku, Sapporo 060-8638, Japan. Email: shime@med.hokudai.ac.jp

Running title: Antitumor CD11b^{+}Ly6G^{+} cells induced by dsRNA

Keywords: Toll-like receptor, tumor-associated myeloid cells, TICAM-1 (TRIF), ROS/RNS, type-I IFNs

Abstract

PolyI:C, a synthetic double-stranded RNA analog, acts as an immune-enhancing adjuvant that regresses tumors via cytotoxic T lymphocyte (CTL)-dependent and CTL-independent fashions, the latter of which remains largely unknown. Tumors contain $CD11b^{+}Ly6G^{+}$ cells, granulocytic myeloid-derived suppressor cells (G-MDSCs), or tumor-associated neutrophils (TANs), which play a critical role in tumor progression and development. Here, we demonstrate that $CD11b^{+}Ly6G^{+}$ cells respond to polyI:C and exhibit tumoricidal activity in an EL4 tumor implant model. PolyI:C-induced inhibition of tumor growth was attributed to caspase-8/3 cascade activation in tumor cells, which occurred independently of $CD8\alpha^{+}/CD103^{+}$ dendritic cells (DCs) and CTLs. $CD11b^{+}Ly6G^{+}$ cells acted as anti-tumor effectors because depletion of $CD11b^{+}Ly6G^{+}$ cells totally abrogated tumor regression and caspase activation after polyI:C treatment. $CD11b^{+}Ly6G^{+}$ cells that had been activated with polyI:C showed cytotoxicity and inhibition of tumor growth through the production of reactive oxygen species (ROS)/reactive nitrogen species (RNS). These responses were abolished in either toll/interleukin-1 receptor domain-containing adaptor molecule-1 $(TICAM\text{-}1)^{-/-}$ or interferon (IFN)-αβ receptor 1 $(IFNAR1)^{-/-}$ mice. Thus, our results suggest that polyI:C targets myeloid cells in tumors, where $CD11b^{+}Ly6G^{+}$ cells exhibit anti-tumor activity through TLR3/TICAM-1 and IFNAR pathways, independent of those in $CD8\alpha^{+}/CD103^{+}$ DCs that prime CTLs.

Introduction

Immune cells are implicated in the regulation of tumor growth [1,2]. Toll-like receptors (TLRs) and other pathogen-recognition receptors (PRRs) in myeloid cells trigger signals for the proliferation of tumor cells and activation of immune-effector cells. Stromal myeloid-derived cells, such as macrophages and dendritic cells (DCs), express a set of TLRs and participate in the formation of tumor-progressive or tumor-suppressive microenvironments in response to PRR stimuli. Inflammatory conditions modified by TLR/PRR stimulators and cytokines critically affect the process of tumorigenesis, as well as evoking antitumor immunity. Intratumor myeloid cells phagocytose tumor debris or exosomes containing tumor-associated antigens (TAAs) to prime antigen-specific cytotoxic T lymphocytes (CTLs) together with released cytokines [2]. Although CTLs are critical for tumor regression, tumor cells do not always generate neoantigens or present TAAs [3,4]. Even under the conditions where CTLs no longer participate in TAA-dependent tumor elimination, TLR adjuvants often induce a tumor-regressive response. Therefore, a CTL-independent antitumor event occurs via stimulation of TLRs in tumor-associated myeloid cells during immunotherapy with an adjuvant. The mechanism of this antitumor response remains largely undetermined.

PolyI:C, a synthetic double-stranded RNA (dsRNA) analog, induces type-I interferon (IFN) production and fosters DC maturation, thereby inhibiting tumor growth by natural killer (NK) cells and CTLs in mice [5,6]. In either case, polyI:C is internalized into myeloid cells and recognized by TLR3 in endosomes [7]. TLR3 activates an adaptor molecule, toll/interleukin-1 receptor domain-containing adaptor molecule-1 (TICAM-1), which evokes the production of type-I IFNs and proinflammatory cytokines in myeloid cells [8]. In most somatic cells including some myeloid cells, polyI:C additionally activates the melanoma differentiation-associated gene 5 (MDA5)-mitochondrial antiviral-signaling protein (MAVS)

pathway in the cytosol [9], which triggers a systemic IFN/cytokine response. These pathways are conserved in most myeloid cells and in part contribute to the formation of anti-tumor immune responses.

Myeloid-derived cells are usually immunosuppressive to support tumor growth, and abnormally accumulate in tumor-bearing hosts. $CD11b^+Ly6G^+$ cells represent a population of tumor-supporting myeloid cells in mice [10]. They reside in tumors and blood/lymphoid organs and promote tumor growth, metastasis, angiogenesis, and immunosuppression [11-14]. $CD11b^+Ly6G^+$ cells are identified as granulocytic myeloid-derived suppressor cells (G-MDSCs) in tumors and peripheral tissues or as tumor-associated neutrophils (TANs) in tumors [10]. G-MDSCs and TANs show morphological and functional similarities to neutrophils in tumor-free mice [15]. In patients, neutrophil infiltration into a tumor is correlated with poor prognosis [16,17].

G-MDSCs preferentially produce reactive oxygen species (ROS) and reactive nitrogen species (RNS) including hydrogen peroxide (H_2O_2) and peroxynitrite (PNT). PNT derived from G-MDSCs is a major effector responsible for the immunosuppressive activity on T cell proliferation, as well as the impairment of antigen presentation by tumor cells [18-21]. Consequently, these suppression mechanisms enable tumor cells to escape tumor antigen-specific CTLs. However, emerging evidence has revealed that functionally polarized neutrophils induced by regulatory molecules including cytokines, chemokines, and growth factors, inhibit tumor growth and metastasis [22-24]. $CD11b^+Ly6G^+$ cells, therefore, have both a positive and negative impact on tumor growth, which can be determined by external stimuli. $CD11b^+Ly6G^+$ cells may act as a CTL-independent effector of tumor regression in response to TLR ligands.

Growth control of tumor cells can be altered by targeting immunosuppressive myeloid cells [25]. Administration of purified ligands for TLR3 as well as TLR9 is useful for inducing a functional conversion of $CD11b^+Gr1^+$ MDSCs or monocytic MDSCs (M-MDSCs; $CD11b^+Ly6G^-Ly6C^{high}$), another subset of

MDSCs, in tumor-bearing mice [26-28]. We have previously demonstrated that a polyI:C-induced TLR3-TICAM-1 signal induces tumoricidal activity in tumor-associated macrophages (TAMs), leading to inhibition of tumor growth in 3LL tumor-bearing mice [29]. These observations suggest that polyI:C may be a good tool for the functional alteration of tumor-associated myeloid cells. In the present study, using an EL4 tumor model, we found that $CD11b^{+}Ly6G^{+}$ cells inhibit tumor growth in polyI:C-treated mice even if tumor cells are out of targets of CTL, NK, and M1 TAM-mediated cytolysis.

Results

Inhibition of tumor growth by polyI:C treatment through the TICAM-1 signaling pathway

The growth of EL4 tumors in mice was significantly retarded by polyI:C administration as early as 2 days post-treatment (Figure 1a). To analyze the host pathway involved in this tumor growth inhibition, EL4 cells were implanted into mice deficient for TICAM-1 or MAVS, which are downstream adapter molecules of TLR3 or MDA5, respectively. Then, knockout (KO) mice were treated with polyI:C and tumor growth rates were compared with those from wild type (WT) mice. The polyI:C-induced inhibition of tumor growth was abrogated in TICAM-$1^{-/-}$ but not $MAVS^{-/-}$ mice (Figure 1a). PoyI:C induced the production of type-I IFNs and suppressed EL4 tumor growth, which was abrogated in $IFNAR1^{-/-}$ mice. Thus, polyI:C treatment led to the inhibition of EL4 tumor growth via the TLR3/TICAM-1 signaling pathway and type-I IFN production. EL4 cells express MHC class-I molecules (H-$2D^b$ and H-$2K^b$), CD3ε, CD28, PD-1, and PD-L1, but not MHC class-II molecules (I-Ab), CD4, CD8, CD11b, CD11c, and CTLA-4 (Supplementary Table 1). EG7 cells expressing a model TAA (OVA protein) are a CTL-sensitive cell line derived from EL4 cells. However, polyI:C-induced inhibition of EL4 tumor growth was not abrogated by pretreatment of mice with antibodies (Abs) against CD8β, CD4, or NK1.1 (Figure 1b). PolyI:C treatment robustly increased TUNEL-positive cells, suggesting that apoptosis or necrosis occurred in the tumor (Figure 1c).

Cleaved caspase-3, an apoptosis marker, [30,31] was increased throughout the tumors in response to polyI:C treatment; this effect was abrogated in TICAM-$1^{-/-}$ and $IFNAR1^{-/-}$, but not $MAVS^{-/-}$ mice (Figure 1d). Caspase-3 activation is induced by caspase-8, 9, and 12 [31]. A cleaved form of caspase-8 was specifically increased in tumor lysates at 7 and 18 h after polyI:C treatment in mice (Figure 1e and 1f). The amount of the full-length caspase-9 slightly decreased at 18 h after polyI:C treatment and the amount of full-length

caspase-12 was unchanged. These data suggest that polyI:C treatment induces apoptosis of EL4 tumor cells through the caspase-8/3 cascade, resulting in the inhibition of tumor growth in mice.

CD11b$^+$Ly6G$^+$ cells are essential for polyI:C-induced inhibition of EL4 tumor growth in mice

The TLR3-TICAM-1 pathway triggers an apoptotic signal in cancer cells through caspase-8 activation, as well as proinflammatory responses in immune cells [32]. However, EL4 cells are insensitive to direct stimulation with polyI:C in culture [33].

The polyI:C-induced caspase-3 activation in tumors occurred similarly in Batf3$^{-/-}$ mice, which lack CD8α$^+$/CD103$^+$ DC subsets [34] (Supplementary Figure 1). Taken together, the CD8α$^+$/CD103$^+$ DC-mediated NK and CTL induction is unlikely involved in the inhibition of EL4 tumor growth. That is, previously unidentified cells and/or mechanisms could participate in the therapeutic potential of polyI:C in the EL4-implant model.

We ultimately found that depletion of Gr1$^+$ cells abolished the polyI:C-induced inhibition of tumor growth (Figure 2a). Gr1 is a common epitope of both Ly6G and Ly6C, which are highly expressed on G-MDSCs/TAN and M-MDSCs, respectively. Treatment of tumor-bearing mice with an Ly6G-specific Ab (1A8) almost completely abrogated both of the polyI:C-induced events: inhibition of tumor growth and caspase-8/3 activation in tumors (Figure 2b and 2c). Ly6G$^+$ cells in tumor and spleen co-expressed CD11b (Supplementary Figure 2). Hence, CD11b$^+$Ly6G$^+$ cells are responsible for the inhibition of EL4 tumor growth in polyI:C-treated mice.

PolyI:C-activated CD11b$^+$Ly6G$^+$ cells inhibit tumor growth

We analyzed the gene expression profile of $CD11b^+Ly6G^+$ cells isolated from tumor-bearing mice. Results showed that IFN-α and IFN-β were upregulated in $CD11b^+Ly6G^+$ cells in response to 4 h polyI:C treatment, an effect that was abrogated in TICAM-$1^{-/-}$ $CD11b^+Ly6G^+$ cells, whereas mRNA expression of neither tumor-supporting factors such as arginase-1 (Arg-1) nor vascular endothelial growth factor A (VEGFA) were altered (Supplementary Figure 3a). Therefore, $CD11b^+Ly6G^+$ cells respond to polyI:C treatment *in vivo* within 4 h to alter their function.

$CD11b^+Gr1^+$ cells isolated from tumor-bearing mice directly promote tumor growth when co-injected with tumor cell lines [35-37]. Thus, we tested whether polyI:C-activated $CD11b^+Ly6G^+$ cells inhibited tumor growth. $CD11b^+Ly6G^+$ cells isolated from tumor-bearing mice pre-treated with polyI:C or PBS (as a control) were mixed with EL4 cells and then implanted subcutaneously (s.c.) into tumor-free mice. When EL4 cells were co-implanted into mice with $CD11b^+Ly6G^+$ cells from PBS-treated tumor-bearing mice, the tumor growth rate was similar to that of EL4 cell-implanted mice (without $CD11b^+Ly6G^+$ cells) (Figure 2d, left). In contrast, tumor growth was significantly delayed when EL4 cells were co-implanted with $CD11b^+Ly6G^+$ cells from polyI:C-treated mice (Figure 2d, left). Thus, polyI:C-activated $CD11b^+Ly6G^+$ cells are sufficient to inhibit tumor growth. In contrast, $CD11b^+Ly6G^+$ cells isolated from tumor-bearing TICAM-$1^{-/-}$ mice pre-treated with polyI:C failed to inhibit tumor growth (Figure 2d, right).

We next asked whether $CD11b^+Ly6G^+$ cells in tumor-bearing mice directly killed EL4 cells. $CD11b^+Ly6G^+$ cells from polyI:C-treated tumor-bearing mice showed higher cytotoxic activity than $CD11b^+Ly6G^+$ cells from PBS-treated mice (Figure 2e, left). $CD11b^+Ly6G^+$ cells isolated from TICAM-$1^{-/-}$ mice did not show this activity (Figure 2e, right).

TNF family receptors do not participate in the inhibition of EL4 tumor growth by polyI:C

Ligand stimulation of tumor necrosis factor (TNF) family receptors, such as TNF receptor-1 (TNFR1), receptors for TNF-related apoptosis-inducing ligand (TRAIL), or Fas induces apoptosis in tumor cells through the activation of caspase-8/3 [30]. PolyI:C enhances the expression of ligands from the TNF receptor family in myeloid-derived cells. Therefore, we tested whether those ligands are involved in the anti-tumor effect of polyI:C. TNF-α, a TNFR1 ligand, did not participate in the polyI:C-induced caspase-3 activation in tumors, as determined from TNFα$^{-/-}$ mice (Supplementary Figure 4a). TNF-α does not induce cell death of EL4 cells *in vitro* [29]. Furthermore, we observed that *in vivo* and *in vitro* polyI:C treatment increased mRNA expression of TRAIL in CD11b^{+}Ly6G^{+} cells (Supplementary Figure 4b). TRAIL exerts cytotoxic activity toward tumor cells such as C1498 cells via DR4 or DR5 receptor stimulation, which induces caspase-8/3 cascade activation *in vitro* [30]. DR5 expression was observed on the surface of EL4 cells (Supplementary Figure 4c). To test whether EL4 cells were sensitive to TRAIL-induced apoptosis, we incubated EL4 and C1498 cells with recombinant TRAIL (rTRAIL). The viability of C1498 cells was decreased by rTRAIL, which was abrogated by a neutralizing Ab. In contrast, the viability of EL4 cells was not affected by treatment with rTRAIL, indicating that EL4 cells were resistant to TRAIL-induced apoptosis, probably due to a functional defect in the intracellular signaling pathway downstream of DR5 (Supplementary Figure 4d). Furthermore, CD11b^{+}Ly6G^{+} cells did not show an increase in the expression levels of FasL after polyI:C treatment (Supplementary Figure 3b). Thus, ligands for the members of the TNF receptor family are not major factors for the inhibition of EL4 tumor growth by polyI:C treatment.

ROS/RNS induce caspase-8/3 activation and EL4 cell death

ROS/RNS, including PNT and H_2O_2, induce apoptosis of cancer cells [38]. When added exogenously, these molecules lead to a specific cell-type activation of multiple caspases such as caspase-8, 9, and 3 [39-41]. As

shown in Supplementary Figure 5, fluorescence levels of 2′,7′-dichlorodihydrofluorescein diacetate (H2DCFDA), a cell-permeant indicator of ROS/RNS, were increased in $CD11b^{+}Gr1^{+}$ cells infiltrating into tumors in response to polyI:C treatment, suggesting that $CD11b^{+}Gr1^{+}$ cells respond to polyI:C to produce ROS/RNS. *In vitro* treatment of EL4 cells with PNT resulted in an increase of apoptosis accompanied with caspase-8/3 activation in EL4 cells (Figure 3a and 3b), which was abrogated by uric acid, a ROS/RNS scavenger (Figure 3c). Other report demonstrated that H_2O_2 induces apoptosis in HeLa cells through the caspase-8/3 cascade, independent of caspase-9 activation [42]. Similar to PNT, H_2O_2 treatment decreased the viability of EL4 cells and induced caspase-3 and caspase-8 activation (Figure 3d and 3e).

Next, we examined the gene expression profile for ROS/RNS production in polyI:C-treated $CD11b^{+}Gr1^{+}$ cells. PNT is formed by a reaction of nitric oxide (NO) with a superoxide anion (O_2^{-}). NO and O_2^{-} are produced by iNOS and a NADPH oxidase 2 (NOX2, $gp91^{phox}$)-containing molecular complex, respectively [38]. As shown in Figure 4a and 4b, polyI:C treatment induced protein and mRNA expression of iNOS in $CD11b^{+}Ly6G^{+}$ cells from the tumor and spleen. iNOS mRNA expression was increased by *in vitro* polyI:C stimulation (Supplementary Figure 6a). Induction of iNOS expression was partially dependent on TICAM-1, because the polyI:C-induced expression of iNOS mRNA was significantly reduced in TICAM-$1^{-/-}$ $CD11b^{+}Ly6G^{+}$ cells (Figure 4b and Supplementary Figure 6a). $CD11b^{+}Ly6G^{+}$ cells highly produce O_2^{-} in response to various types of stimuli through the activation of the NADPH oxidase complex localized in the plasma membrane. A similar result was observed for the expression of the NOX2 gene (Figure 4b).

To verify that $CD11b^{+}Ly6G^{+}$ cells produce PNT in response to polyI:C treatment *in vivo*, we stained $CD11b^{+}Ly6G^{+}$ cells with aminophenyl fluorescein (APF) and hydroxyphenyl fluorescein (HPF), the cell permeable fluorescent probes for the detection of ROS/RNS. APF detects hydroxyl radicals (•OH), peroxynitrite ions (PNT, $ONOO^{-}$), and hypochlorite ions (OCl^{-}). HPF detects PNT and OCl^{-}, but rarely reacts

with other ROS/RNS including O_2^-, H_2O_2, and NO. The frequency of $CD11b^+Ly6G^+$ cells with increased fluorescence, representing an enhanced ROS/RNS production, was increased in tumor and spleen at 7 h after polyI:C treatment *in vivo* (Figure 4c and Supplementary Figure 6b). This response was specific to $CD11b^+Ly6G^+$ cells in both tumor and spleen because polyI:C treatment barely affected the fluorescence intensity of $Ly6G^-$ populations. To determine whether $CD11b^+Ly6G^+$ cells produce PNT in response to polyI:C treatment, an iNOS inhibitor, which blocks NO production, was added to tumor-bearing mice to inhibit the enzymatic activity of iNOS. The increase in the fluorescence intensity of APF-stained $CD11b^+Ly6G^+$ cells was largely attenuated in tumor-bearing mice treated with N^G-nitro-L-arginine methyl ester (L-NAME), an iNOS inhibitor (Figure 4d), suggesting that $CD11b^+Ly6G^+$ cells produced PNT in response to polyI:C stimulation. The APF fluorescence of TICAM-$1^{-/-}$ $CD11b^+Ly6G^+$ cells was barely increased by treatment with polyI:C *in vivo* (Figure 4e and Supplementary Figure 6b), although iNOS mRNA remained slightly expressed (Figure 4b). Similar results were obtained when splenocytes of tumor-bearing mice were activated with polyI:C *in vitro* (Supplementary Figure 6c). TICAM-1-dependent PNT production in activated $CD11b^+Ly6G^+$ cells was confirmed by HPF staining (Figure 4f).

We then examined the response of $CD11b^+Ly6G^+$ cells to polyI:C treatment in IFNAR$1^{-/-}$ mice. PolyI:C treatment did not induce ROS/RNS production in tumor-infiltrated $CD11b^+Ly6G^+$ cells from IFNAR$1^{-/-}$ mice (Figure 4g). PolyI:C treatment induced mRNA expression of type-I IFNs by $CD11b^+Ly6G^+$ cells in tumor-bearing mice, which was dependent on the TICAM-1 pathway (Supplementary Figure 3a). Recombinant type-I IFNs increased the production of ROS/RNS by $CD11b^+Ly6G^+$ cells (Supplementary Figure 7). Tumor-infiltrating $CD11b^+Ly6G^+$ cells also showed enhanced H_2O_2 production after polyI:C treatment (Figure 4h).

ROS/RNS are responsible for the anti-tumor activity of polyI:C-activated CD11b$^+$Ly6G$^+$ cells

Next, we determined whether ROS/RNS were involved in the tumor growth inhibition of EL4 cells by polyI:C-activated CD11b$^+$Ly6G$^+$ cells. We performed a co-implantation experiment (as in Figure 2d) to evaluate the possibility that ROS/RNS are effectors of polyI:C-activated CD11b$^+$Ly6G$^+$ cells. Mice were treated with uric acid or L-NAME after co-implantation of EL4 cells with CD11b$^+$Ly6G$^+$ cells. CD11b$^+$Ly6G$^+$ cell-induced inhibition of tumor growth was abrogated in mice treated with both reagents (Figure 5a and 5b). Furthermore, N6-(1-Iminoethyl)-L-lysine dihydrochloride (L-NIL; iNOS inhibitor) inhibited the cytotoxic activity of CD11b$^+$Ly6G$^+$ cells even after polyI:C activation (Figure 5c). ROS/RNS production by polyI:C-activated CD11b$^+$Ly6G$^+$ cells is required for exertion of their anti-tumor activity.

PNT and H_2O_2 induce caspase-8/3 activation and cell death in cancer cell lines

We investigated whether CD11b$^+$Ly6G$^+$ cells were generally important for tumor growth inhibition by polyI:C treatment using another tumor model. Inhibition of B16 tumor growth is largely dependent on NK cells in polyI:C therapy [5]. The inhibitory effect of polyI:C on B16 tumor growth was partially abrogated in mice pretreated with an anti-Ly6G Ab (Figure 6a). CD11b$^+$Ly6G$^+$ cells activated by polyI:C inhibited tumor growth of B16 cells in mice (Figure 6b). Furthermore, polyI:C induced ROS/RNS production from CD11b$^+$Ly6G$^+$ cells in tumor and spleen of mice implanted with B16, and also 3LL, and MC38 cells (Figure 6c and Supplementary Figure 8).

Next, to determine whether ROS/RNS induce caspase-8/3 activation and cytotoxicity in those cancer cell lines, we treated them with PNT and examined the cytotoxicity (Figure 6d). B16 cells were also treated with H_2O_2 (Figure 6e). PNT and H_2O_2 exerted cytotoxicity against 3LL cells and B16 cells, as well as EL4 cells (Figure 6d and 6e); caspase-8/3 activation was also induced in these cell lines (Figure 6f). Although

caspase activation was induced, MC38 cells were resistant to PNT-induced cell death. Among them, EL4 cells showed the highest sensitivity to both cytotoxicity and caspase-8/3 activation induced by PNT or H_2O_2 (Figure 3d and 6b). EL4 cells highly expressed caspase-8 mRNA, compared with the other cell lines (Supplementary Figure 9).

EL4 cells enhance PNT production by CD11b$^+$Ly6G$^+$ cells

After *in vitro* polyI:C stimulation, CD11b$^+$Ly6G$^+$ cells showed lower PNT production than those after *in vivo* stimulation (Figure 4f and 7a). Cancer cell-derived factors appear to modulate neutrophil function [43]. Thus, PNT levels in CD11b$^+$Ly6G$^+$ cells induced by polyI:C were measured in the presence of EL4 cells. Basal and polyI:C-induced PNT levels in CD11b$^+$Ly6G$^+$ cells were significantly increased by co-existing EL4 cells compared with CD11b$^+$Ly6G$^+$ cells alone (Figure 7a). EL4 cells secrete granulocyte macrophage colony-stimulating factor (GM-CSF), a known survival factor of G-MDSCs or neutrophils [44]. However, in the presence of recombinant GM-CSF, polyI:C stimulation did not significantly increase PNT production by CD11b$^+$Ly6G$^+$ cells, although the basal levels of ROS/RNS production were increased (Figure 7a). EL4 cells failed to enhance PNT production by CD11b$^+$Ly6G$^+$ cells in a transwell, suggesting that cell-to-cell contact is required for this activity (Figure 7b). Thus, EL4 cells enhance ROS/RNS production by CD11b$^+$Ly6G$^+$ cells probably through stimulation of cell surface molecules that could increase the response of CD11b$^+$Ly6G$^+$ cells to polyI:C. This could explain why EL4 tumors are highly susceptible to CD11b$^+$Ly6G$^+$ cell-mediated anti-tumor activity of polyI:C treatment, in addition to their high sensitivity to ROS/RNS-induced apoptosis.

Discussion

MHC class-I^{high} tumor cells are usually a target for TAA-specific CTLs. PolyI:C enhances cross-priming of CTLs by DCs, and PD-1/PD-L1 regulates tumor cytolysis by effector CTLs. In this study, we found that CD11b^{+}Ly6G^{+} cells, but not CD8 $^{+}$ T cells, act as an effector for the polyI:C-induced tumor growth inhibition in the MHC class-I^{high} EL4 tumor implant model. The TICAM-1-IFNAR pathway is crucial to evoke the anti-tumor activity of CD11b^{+}Ly6G^{+} cells through ROS/RNS production upon polyI:C treatment. This mechanism is different from the one mediated by TAMs, which is also activated through the same signaling pathway, as observed in the 3LL tumor model. CD11b^{+}Ly6G^{+} cells generally produced ROS/RNS in response to polyI:C treatment in mice implanted with various types of tumor cell lines. However, the response does not always lead to tumor regression due to the relatively strong tumoricidal activity of other anti-tumor effector cells, which may cause invisible tumor shrinkage by CD11b^{+}Ly6G^{+} cells. The TICAM-1-IFNAR pathway induces not only DC-primed CTLs, but also cytotoxicity of CD11b^{+}Ly6G^{+} cells against MHC class I ^{high} EL4 lymphoma; this is also seen with MHC class I-negative B16 melanoma. TICAM-1 in myeloid cells is a critical molecule for the antitumor immune activation encompassing DCs, TAMs, and tumor-associated CD11b^{+}Ly6G^{+} cells.

Functional alterations of TAMs and MDSCs have shown to have both positive and negative impacts on tumor growth [45,46]. TLRs could become targets for rendering the phenotype of intratumor myeloid cells from immunosuppressive to tumor-inhibiting [47,48]. MDSCs express an array of TLRs and their activation affects expansion and function of MDSCs. TLR2 or TLR4 activation may accelerate the development of severe immunosuppressive conditions [48,49]. In contrast, activation of TLR9, TLR3, or MDA5 abolishes the suppressive activity of MDSCs and may contribute to tumor growth inhibition [26-28]. In the present study, we demonstrate that TICAM-1 is a critical adapter that determines the anti-tumor activity of CD11b^{+}Ly6G^{+} cells

in RNA adjuvant therapy, and that both TICAM-1-inducible genes and TICAM-1-induced type-I IFNs are important for this anti-tumor mechanism. In combination with our previous data, we propose that myeloid cells expanded in cancer contribute to tumor growth inhibition, particularly under an RNA adjuvant treatment, rather than preventing the therapeutic effects through their immunosuppressive activity. This could be achieved by functional alteration of tumor-associated myeloid cells to exhibit tumor-killing activity. In this context, an RNA adjuvant can induce tumor regression even if immunosuppressive myeloid cells abundantly accumulate in tumors, such that the CTL response is insufficient to regress the tumor.

Cleavage of caspase-8/3, which is triggered by extracellular stimuli [30,31], is a hallmark of apoptosis. We found that the caspase-8/3 cascade is specifically activated in tumors after polyI:C treatment. Excessive amounts of intrinsic, as well as extrinsic ROS/RNS including PNT and H_2O_2, are known to induce activation of the caspase-8/3 cascade in cancer cells, leading to apoptosis [40,41]. We show that $CD11b^+Ly6G^+$ cells produce ROS/RNS including PNT and H_2O_2, in response to polyI:C stimulation both *in vivo* and *in vitro*. PNT and H_2O_2 efficiently induce the activation of the caspase-8/3 cascade and apoptosis of EL4 cells. Inducing cytotoxicity by ROS/RNS treatment in other tumor cell lines such as 3LL and B16 cells (but not MC38 cells) suggests that the susceptibility of tumors to the effector produced by $CD11b^+Ly6G^+$ cells depends on the cancer cell type. Among the cell lines tested, EL4 cells showed the highest sensitivity to PNT- or H_2O_2-induced apoptosis *in vitro*. The high sensitivity of EL4 cells to ROS/RNS may be explained by the fact that the mRNA levels of caspase-8 are relatively high in EL4 cells. Furthermore, polyI:C-induced activation of $CD11b^+Ly6G^+$ cells was supported by EL4 cells, suggesting that the tumor microenvironment is favorable for the activation of $CD11b^+Ly6G^+$ cells. Thus, $CD11b^+Ly6G^+$ cells play a critical role in the inhibition of EL4 tumor growth by polyI:C treatment, which is independent of CTLs. The anti-tumor activity of polyI:C-activated $CD11b^+Ly6G^+$ cells was abrogated by treatment of mice with uric acid or iNOS

inhibitors. Because these reagents neutralize a broad range of ROS/RNS, other ROS/RNS may be synergistically involved in this cytotoxic effect [50-52].

We demonstrate that ROS/RNS production by $CD11b^+Ly6G^+$ cells requires the activation of TICAM-1-IFNAR signaling pathways. This response is partly mediated by TICAM-1-regulated induction of iNOS (NOS2) and NOX2 (Cybb) mRNA expression. ROS/RNS production is regulated by not only iNOS and NOX2 gene expression but also by protein-protein interactions in the TLR3-TICAM-1 signaling pathway [53-55]. Furthermore, our data indicate that TICAM-1-dependent type-I IFN production is critical for ROS/RNS production as well as retardation of tumor growth by $CD11b^+Ly6G^+$ cells activated by polyI:C. The TICAM-1 and IFNAR pathways may cooperatively regulate the expression and activation of iNOS and NADPH oxidase complex. Further studies are required to identify the critical factor to control ROS/RNS production triggered by the TICAM-1-IFNAR pathway in $CD11b^+Ly6G^+$ cells.

Activation of TLR3-TICAM-1 pathway induces multifarious effector mechanisms for tumor regression in which NK cells, CTLs, and M1-shifted TAMs are involved [5,6,29]. In the present study, we further identified $CD11b^+Ly6G^+$ cells as a tumoricidal effector toward some types of tumors. As dsRNA treatment simultaneously induces activation of these effector cells, the sensitivity of cancer cells to the effector molecules ultimately determines each effector cell-mediated tumor clearance. Tumors generally consist of non-parenchymal and parenchymal cells, the latter contains heterogeneous populations of cancer cells with variable phenotypes and likely becomes a target of different types of effector cells, effector molecules, or therapeutic reagents for immunotherapy [56]. Therefore, induction of $CD11b^+Ly6G^+$ cell-mediated cytolysis by dsRNA treatment in combination with other therapies using monoclonal Abs targeting cancer-associated molecules, immune checkpoint inhibitors, or $CD8^+$ T cell-based therapy may be beneficial in some patients.

We propose that the formation of a tumor-suppressive microenvironment is fundamentally induced by the

TLR3-TICAM-1 pathway in myeloid cells, and this pathway is a promising target for the development of cancer immunotherapy.

Materials and Methods

Mice and tumor cells

Inbred C57BL/6 wild-type (B6 WT) mice were purchased from Clea Japan. TICAM-1$^{-/-}$ and MAVS (IPS-1)$^{-/-}$ mice were generated in our laboratory [5,57]. IFNAR1$^{-/-}$ mice were obtained from Dr. T. Taniguchi (University of Tokyo). Mice (aged 6 to 10 weeks) were used in all experiments and maintained under specific pathogen-free conditions. The protocol was approved by the Committee on the Ethics of Animal Experiments in the Animal Safety Center, Hokkaido University, Japan. All mice were used according to the guidelines of the Institutional Animal Care and Use Committee of Hokkaido University, who approved this study as ID number 08-0290 and 13-0043. EL4 cells were obtained from Dr. Sato (Sapporo Medical University). The B16D8 cell line was established in our laboratory as a sub-line of B16 melanoma[58]. 3LL, MC38, and C1498 cell lines were purchased from ATCC (American Type Culture Collection). EL4, B16D8, 3LL, and C1498 cells were cultured at 37 ºC under 5% CO_2 in RPMI1640 medium supplemented with 10% fetal bovine serum (FBS), 100 U/mL penicillin, and 100 µg/mL streptomycin. MC38 cells were cultured in RPMI1640 medium supplemented with 10% FBS, 50 µM 2-ME, 2 mM L-glutamine, 1 mM sodium pyruvate, 100 U/mL penicillin, and 100 µg/mL streptomycin (Life technologies).

Tumor challenge and polyI:C treatment

Mice were shaved at the back and injected s.c. with EL4 cells (1 x 10^6), B16D8 cells (6 x 10^5), 3LL cells (1 x 10^6), or MC38 cells (1 x 10^6) resuspended in 200 µL of PBS(-). Tumor size was measured using a caliper. Tumor volume was calculated using the following formula: tumor volume (cm^3) = (long diameter) x (short diameter)^2 x 0.4. PolyI:C (GE Bioscience) with no detectable LPS was injected s.c. (100 µg/head) or intraperitoneally (i.p.) (200 µg/head). When the tumors reached an average volume of 0.4–0.6 cm^3, the

treatment was started and repeated every 4 days. In some experiments, $Ly6G^+$ cells (1×10^6) isolated from the spleen of tumor-bearing mice (4 h pre-treatment with polyI:C) were mixed with EL4 cells (0.5×10^6) in 200 µL of PBS(-), and then implanted s.c. into tumor-free B6 WT mice. Uric acid (20 mg/head; Sigma-Aldrich) or L-NAME (1.5 mg/head; Sigma-Aldrich) were injected i.p. into tumor-bearing mice after implantation of the cell mixture.

Immunohistochemistry

Tumors were fixed with 10% neutralized buffered formalin at 4 °C for 4 h, equilibrated with 15% sucrose in PBS(-) for 1 h, and then with 30% sucrose in PBS(-) for 16–18 h. Tissue samples were embedded in Tissue Tek^R O.C.T compound (Sakura Finetek Japan), frozen, and stored at -80 °C until use. The tissue block was cut at a thickness of 10 µm. For the terminal deoxynucleotidyl transferase-mediated nick end labeling (TUNEL) assay, tumor sections were stained using the In Situ Cell Death Detection Kit, Fluorescein (Roche). For detection of caspase-3 activation, Abs against cleaved caspase-3 (Asp175) (5A1E) and an Alexa488-anti-rabbit IgG secondary Ab (Life technologies) were used.

Cell isolation and culture

$CD11b^+Ly6G^+$ cells were isolated from a single cell suspension from the spleen of polyI:C- or PBS-injected mice by using a biotin-conjugated anti-Ly6G monoclonal Ab (1A8) (Biolegend) and Streptavidin Microbeads (Miltenyi) according to the manufacturer's instructions. In these purification steps, two rounds of positive selection were performed to increase purity. We routinely prepared $Ly6G^+$ cells at more than 95% purity and almost 100% of $Ly6G^+$ cells expressed CD11b (Supplementary Figure 2). Isolated $CD11b^+Ly6G^+$ cells were cultured in Opti-MEM (Life technologies) supplemented with or without 0.5% FBS for *in vitro*

polyI:C stimulation or cytotoxicity assays, respectively. To inhibit iNOS activity, EL4 tumor-bearing mice were injected i.p. with L-NAME (1.5 mg/head) or L-NIL (0.5 mg/head) 5 h after polyI:C treatment. After 2 h, $CD11b^{+}Ly6G^{+}$ cells were isolated from the spleen and used for the cytotoxicity assay.

Flow cytometry

Single cell suspensions isolated from tumors or spleens were stained with fluorescent dye-labeled Abs after blockade with an anti-CD16/32 Ab (93). The following Abs were used: FITC-anti-CD11b (M1/70), PE-anti-GR1 (RB6-8C5), APC- or FITC-anti-Ly6G (1A8), FITC-anti-CD11c (N418), PE- or APC-anti-F4/80 (BM8), PE-anti-NK1.1 (PK136), PE-anti-CD49b (DX5), PE-anti-CD3e (145-2C11), FITC-anti-CD4 (GK1.5), FITC-anti-CD8a (53-6.7), and PE-anti-CD19 (MB19-1) (eBioscience or Biolegend). For detection of intracellular ROS/RNS, fluorescent probes were applied. Cells were stained with 5 μM APF, 5 μM HPF (SEKISUI Medical), 5 μM BES-H_2O_2-Ac (Wako) at 25 °C for 15 min, followed by staining with an APC-anti-Ly6G Ab (1A8) at 25 °C for 15 min. Samples were analyzed by a FACS Calibur or FACS Aria II (BD Bioscience); data analysis was performed using Flow Jo (Tree star).

***In vivo* depletion**

In vivo depletion of cells was achieved by i.p. injection of ascites containing monoclonal Abs against CD8β (53-6.7), CD4 (GK1.5), NK1.1 (PK136), or Gr1 (RB6-8C5). For $Ly6G^{+}$ cell depletion, 150 μg of Ultra-LEAF purified anti-mouse Ly6G Ab (1A8) (Biolegend) was injected i.p. into mice. Ultra-LEAF purified rat IgG2a (Biolegend) was used as an isotype matched control Ab. Antibodies were injected 1 day before the polyI:C treatment. Depletion of cells in tumor-bearing mice was confirmed by flow cytometry of spleen and tumor cell suspensions.

Immunoblotting

Tumors excised from mice or cancer cell lines were lysed in 1% NP-40, 10 mM Tris-HCl (pH 7.2) supplemented with a complete protease inhibitor cocktail (Roche) and incubated for 30 min on ice. The lysate was centrifuged at 15 000 rpm for 10 min to remove cell debris. The supernatant was mixed with a 2x SDS-PAGE sample buffer and heated at 85 °C for 5 min. Samples were stored at -30 °C until use. An equal amount (50 μg) of protein was analyzed by SDS-PAGE (12% acrylamide). Abs against cleaved caspase-3 (Asp175) (5A1E), cleaved caspase-8 (Asp387), full-length caspase-9, full-length caspase-12 (Cell Signaling Technology), and HRP-conjugated goat anti-rabbit IgG Ab (Life technologies) were used for detection of caspases.

Cytotoxic activity assay

Cytotoxic activity of $CD11b^{+}Ly6G^{+}$ cells was measured by the following procedure. EL4 cells (1×10^{6}) were incubated in 1 mL of 0.5 μM carboxyfluorescein diacetate succinimidyl ester (CFSE) in PBS at 37 °C for 15 min. After washing 2 times with RPMI1640 supplemented with 10% FBS, CFSE-labeled EL4 cells were cultured in Opti-MEM (Life technologies) containing 10 ng/mL recombinant mouse GM-CSF (Peprotech) for 4 h. $CD11b^{+}Ly6G^{+}$ cells were isolated from the spleen of tumor-bearing mice, suspended in Opti-MEM, and mixed with CFSE-labeled EL4 cells. After 20–24 h incubation, dead cells were detected with the SYTOX AADvanced Dead Cell Stain (Life technologies) according to the manufacturer's instructions. The proportion of dead cells in $CFSE^{+}$ cells (EL4 cells) was measured by FACS Calibur or FACS Aria II. Cytotoxicity percentage was calculated with the following formula: [(Live cell %/Dead cell% effector) –

(Live cell%/Dead cell% control)] x 100. WST-1 assay was performed according to the manufacturer's instructions (Dojindo).

RNA isolation and RT-PCR analysis

Total RNA from $CD11b^{+}Ly6G^{+}$ cells was isolated with the TRIzol reagent (Life technologies) or the RNeasy mini kit (QIAGEN) according to the manufacturer's instructions. Complementary DNA (cDNA) was synthesized using a High-Capacity cDNA Reverse Transcription Kit (Applied Biosystems). Real-time PCR was performed with Power SYBR Green PCR Master Mix (Applied Biosystems) and a StepOne Real-Time PCR System (Applied Biosystems). Expression of the cytokine genes was normalized to the expression of mouse glyceraldehyde 3-phosphate dehydrogenase (GAPDH). We used following primer pairs: mouse GAPDH forward, 5′-GCCTGGAGAAACCTGCCA-3′, GAPDH reverse, 5′-CCCTCAGATGCCTGCTTCA-3′; mouse iNOS (NOS2) forward, 5′-CAGCTGGGCTGTACAAACCTTC-3′, mouse iNOS (NOS2) reverse, 5′-CATTGGAAGTGAAGCGTTTCG-3′; mouse NOX2 (pg91phox, Cybb) forward, 5′-TGCAGTGCTATCATCCAAGC-3′, mouse NOX2 (pg91phox, Cybb) reverse, 5'-CTTTCTCAGGGGTTCCAGTG-3'. Data were analyzed by the ΔΔCt method.

Statistical analysis

Statistically significant differences between two groups were determined using the Student's t-test.

Acknowledgements

We are grateful to our laboratory members for their invaluable discussions. We also thank Dr T. Taniguchi (University of Tokyo) for providing IFNAR1$^{-/-}$ mice. This work was supported by JSPS KAKENHI Grant Numbers, 24590470, and16K08704, Grants from the The Ministry of Health, Labour and Welfare (MHLW) and the Research on Development of New Drugs, the Japan Agency for Medical Research and Development (AMED) (16ak0101010h0005), the Takeda Science Foundation, and the Kato memorial bioscience foundation.

Competing financial interests

The authors declare no competing financial interests.

Supplementary information is available at Cell Death and Differentiation's website.

References

1 Hanahan D, Coussens LM. Accessories to the Crime: Functions of Cells Recruited to the Tumor Microenvironment. *Cancer Cell* 2012; **21**: 309–322.

2 Gajewski TF, Schreiber H, Fu Y-X. Innate and adaptive immune cells in the tumor microenvironment. *Nat Immunol* 2013; **14**: 1014–1022.

3 Pardoll DM. The blockade of immune checkpoints in cancer immunotherapy. *Nat Rev Cancer* 2012; **12**: 252–264.

4 Marabelle A, Kohrt H, Caux C, Levy R. Intratumoral immunization: a new paradigm for cancer therapy. *Clin Cancer Res* 2014; **20**: 1747–1756.

5 Akazawa T, Ebihara T, Okuno M, Okuda Y, Shingai M, Tsujimura K *et al.* Antitumor NK activation induced by the Toll-like receptor 3-TICAM-1 (TRIF) pathway in myeloid dendritic cells. *Proc Natl Acad Sci USA* 2007; **104**: 252–257.

6 Azuma M, Ebihara T, Oshiumi H, Matsumoto M, Seya T. Cross-priming for antitumor CTL induced by soluble Ag + polyI:C depends on the TICAM-1 pathway in mouse CD11c(+)/CD8α(+) dendritic cells. *Oncoimmunol* 2012; **1**: 581–592.

7 Matsumoto M, Funami K, Tanabe M, Oshiumi H, Shingai M, Seto Y *et al.* Subcellular localization of Toll-like receptor 3 in human dendritic cells. *J Immunol* 2003; **171**: 3154–3162.

8 Oshiumi H, Matsumoto M, Funami K, Akazawa T, Seya T. TICAM-1, an adaptor molecule that participates in Toll-like receptor 3-mediated interferon-beta induction. *Nat Immunol* 2003; **4**: 161–167.

9 McCartney S, Vermi W, Gilfillan S, Cella M, Murphy TL, Schreiber RD *et al.* Distinct and complementary functions of MDA5 and TLR3 in poly(I:C)-mediated activation of mouse NK cells. *J Exp Med* 2009; **206**: 2967–2976.

10 Gabrilovich DI, Ostrand-Rosenberg S, Bronte V. Coordinated regulation of myeloid cells by tumours. *Nat Rev Immunol* 2012; **12**: 253–268.

11 Pekarek LA, Starr BA, Toledano AY, Schreiber H. Inhibition of tumor growth by elimination of granulocytes. *J Exp Med* 1995; **181**: 435–440.

12 Nozawa H, Chiu C, Hanahan D. Infiltrating neutrophils mediate the initial angiogenic switch in a mouse model of multistage carcinogenesis. *Proc Natl Acad Sci USA* 2006; **103**: 12493–12498.

13 Shojaei F, Wu X, Qu X, Kowanetz M, Yu L, Tan M *et al.* G-CSF-initiated myeloid cell mobilization and angiogenesis mediate tumor refractoriness to anti-VEGF therapy in mouse models. *Proc Natl Acad Sci USA* 2009; **106**: 6742–6747.

14 Nagaraj S, Collazo M, Gabrilovich DI. Subsets of myeloid-derived suppressor cells in tumor-bearing mice. *J Immunol* 2008; **181**: 5791–5802.

15 Dumitru CA, Lang S, Brandau S. Modulation of neutrophil granulocytes in the tumor microenvironment: mechanisms and consequences for tumor progression. *Semin Cancer Biol* 2013; **23**: 141–148.

16 Reid MD, Basturk O, Thirabanjasak D, Hruban RH, Klimstra DS, Bagci P *et al.* Tumor-infiltrating neutrophils in pancreatic neoplasia. *Mod Pathol* 2011; **24**: 1612–1619.

17 Donskov F, Maase von der H. Impact of immune parameters on long-term survival in metastatic renal cell carcinoma. *J Clin Oncol* 2006; **24**: 1997–2005.

18 Corzo CA, Cotter MJ, Cheng P, Cheng F, Kusmartsev S, Sotomayor E *et al.* Mechanism regulating reactive oxygen species in tumor-induced myeloid-derived suppressor cells. *J Immunol* 2009; **182**: 5693–5701.

19 Raber PL, Thevenot P, Sierra R, Wyczechowska D, Halle D, Ramirez ME *et al.* Subpopulations of myeloid-derived suppressor cells impair T cell responses through independent nitric oxide-related pathways. *Int J Cancer* 2013; **134**: 2853–2864.

20 Nagaraj S, Gupta K, Pisarev V, Kinarsky L, Sherman S, Kang L *et al.* Altered recognition of antigen is a mechanism of CD8+ T cell tolerance in cancer. *Nat Med* 2007; **13**: 828–835.

21 Lu T, Ramakrishnan R, Altiok S, Youn J-I, Cheng P, Celis E *et al.* Tumor-infiltrating myeloid cells induce tumor cell resistance to cytotoxic T cells in mice. *J Clin Invest* 2011; **121**: 4015–4029.

22 Fridlender ZG, Sun J, Kim S, Kapoor V, Cheng G, Ling L *et al.* Polarization of tumor-associated neutrophil phenotype by TGF-beta: "N1" versus 'N2' TAN. *Cancer Cell* 2009; **16**: 183–194.

23 Granot Z, Henke E, Comen EA, King TA, Norton L, Benezra R. Tumor entrained neutrophils inhibit seeding in the premetastatic lung. *Cancer Cell* 2011; **20**: 300–314.

24 Finisguerra V, Di Conza G, Di Matteo M, Serneels J, Costa S, Thompson AAR *et al.* MET is required for the recruitment of anti-tumoural neutrophils. *Nature* 2015; **522**: 349–353.

25 Noy R, Pollard JW. Tumor-Associated Macrophages: From Mechanisms to Therapy. *Immunity* 2014; **41**: 49–61.

26 Zoglmeier C, Bauer H, Nörenberg D, Wedekind G, Bittner P, Sandholzer N *et al.* CpG blocks immunosuppression by myeloid-derived suppressor cells in tumor-bearing mice. *Clin Cancer Res* 2011; **17**: 1765–1775.

27 Shirota Y, Shirota H, Klinman DM. Intratumoral injection of CpG oligonucleotides induces the differentiation and reduces the immunosuppressive activity of myeloid-derived suppressor cells. *J Immunol* 2012; **188**: 1592–1599.

28 Shime H, Kojima A, Maruyama A, Saito Y, Oshiumi H, Matsumoto M *et al.* Myeloid-Derived Suppressor Cells Confer Tumor-Suppressive Functions on Natural Killer Cells via Polyinosinic:Polycytidylic Acid Treatment in Mouse Tumor Models. *J Innate Immun* 2014; **6**: 293–305.

29 Shime H, Matsumoto M, Oshiumi H, Tanaka S, Nakane A, Iwakura Y *et al.* Toll-like receptor 3 signaling converts tumor-supporting myeloid cells to tumoricidal effectors. *Proc Natl Acad Sci USA* 2012; **109**: 2066–2071.

30 Crowder RN, El-Deiry WS. Caspase-8 regulation of TRAIL-mediated cell death. *Exp Oncol* 2012; **34**: 160–164.

31 Olsson M, Zhivotovsky B. Caspases and cancer. *Cell Death Differ* 2011; **18**: 1441–1449.

32 Estornes Y, Toscano F, Virard F, Jacquemin G, Pierrot A, Vanbervliet B *et al.* dsRNA induces apoptosis through an atypical death complex associating TLR3 to caspase-8. *Cell Death Differ* 2012; **19**: 1482–1494.

33 Takemura R, Takaki H, Okada S, Shime H, Akazawa T, Oshiumi H *et al.* PolyI:C-Induced, TLR3/RIP3-Dependent Necroptosis Backs Up Immune Effector-Mediated Tumor Elimination In Vivo. *Cancer Immunology Research* 2015; **3**: 902–914.

34 Hildner K, Edelson BT, Purtha WE, Diamond M, Matsushita H, Kohyama M *et al.* Batf3 deficiency reveals a critical role for CD8alpha+ dendritic cells in cytotoxic T cell immunity. *Science* 2008; **322**: 1097–1100.

35 Yang L, DeBusk LM, Fukuda K, Fingleton B, Green-Jarvis B, Shyr Y *et al.* Expansion of myeloid immune suppressor Gr+CD11b+ cells in tumor-bearing host directly promotes tumor angiogenesis. *Cancer Cell* 2004; **6**: 409–421.

36 Shojaei F, Wu X, Malik AK, Zhong C, Baldwin ME, Schanz S *et al.* Tumor refractoriness to anti-VEGF treatment is mediated by CD11b+Gr1+ myeloid cells. *Nat Biotechnol* 2007; **25**: 911–920.

37 Ren G, Zhao X, Wang Y, Zhang X, Chen X, Xu C *et al.* CCR2-Dependent Recruitment of Macrophages by Tumor-Educated Mesenchymal Stromal Cells Promotes Tumor Development and Is Mimicked by TNFα. *Cell Stem Cell* 2012; **11**: 812–824.

38 Szabó C, Ischiropoulos H, Radi R. Peroxynitrite: biochemistry, pathophysiology and development of therapeutics. *Nat Rev Drug Discov* 2007; **6**: 662–680.

39 Walford GA, Moussignac R-L, Scribner AW, Loscalzo J, Leopold JA. Hypoxia potentiates nitric oxide-mediated apoptosis in endothelial cells via peroxynitrite-induced activation of mitochondria-dependent and -independent pathways. *J Biol Chem* 2004; **279**: 4425–4432.

40 Zhuang S, Simon G. Peroxynitrite-induced apoptosis involves activation of multiple caspases in HL-60 cells. *Am J Physiol, Cell Physiol* 2000; **279**: C341–51.

41 Shacka JJ, Sahawneh MA, Gonzalez JD, Ye Y-Z, D'Alessandro TL, Estévez AG. Two distinct signaling pathways regulate peroxynitrite-induced apoptosis in PC12 cells. *Cell Death Differ* 2006; **13**: 1506–1514.

42 Wu Y, Wang D, Wang X, Wang Y, Ren F, Chang D *et al.* Caspase 3 is Activated through Caspase 8 instead of Caspase 9 during H2O2-induced Apoptosis in HeLa Cells. *Cell Physiol Biochem* 2011; **27**: 539–546.

43 Fridlender ZG, Albelda SM. Tumor-associated neutrophils: friend or foe? *Carcinogenesis* 2012; **33**: 949–955.

44 Chalmin F, Ladoire S, Mignot G, Vincent J, Bruchard M, Remy-Martin J-P *et al.* Membrane-associated Hsp72 from tumor-derived exosomes mediates STAT3-dependent immunosuppressive function of mouse and human myeloid-derived suppressor cells. *J Clin Invest* 2010; **120**: 457–471.

45 Yang W-C, Ma G, Chen S-H, Pan P-Y. Polarization and reprogramming of myeloid-derived suppressor cells. *J Mol Cell Biol* 2013; **5**: 207–209.

46 Quail DF, Joyce JA. Microenvironmental regulation of tumor progression and metastasis. *Nat Med* 2013; **19**: 1423–1437.

47 Yu L, Wang L, Chen S. Dual character of Toll-like receptor signaling: pro-tumorigenic effects and anti-tumor functions. *Biochim Biophys Acta* 2013; **1835**: 144–154.

48 Bunt SK, Clements VK, Hanson EM, Sinha P, Ostrand-Rosenberg S. Inflammation enhances myeloid-derived suppressor cell cross-talk by signaling through Toll-like receptor 4. *J Leukoc Biol* 2009; **85**: 996–1004.

49 Maruyama A, Shime H, Takeda Y, Azuma M, Matsumoto M, Seya T. Pam2 lipopeptides systemically increase myeloid-derived suppressor cells through TLR2 signaling. *Biochem Biophys Res Commun* 2015; **457**: 445–450.

50 Hooper DC, Spitsin S, Kean RB, Champion JM, Dickson GM, Chaudhry I *et al.* Uric acid, a natural scavenger of peroxynitrite, in experimental allergic encephalomyelitis and multiple sclerosis. *Proc Natl Acad Sci USA* 1998; **95**: 675–680.

51 Balavoine GG, Geletii YV. Peroxynitrite scavenging by different antioxidants. Part I: convenient assay. *Nitric Oxide* 1999; **3**: 40–54.

52 Hooper DC, Scott GS, Zborek A, Mikheeva T, Kean RB, Koprowski H *et al.* Uric acid, a peroxynitrite scavenger, inhibits CNS inflammation, blood-CNS barrier permeability changes, and tissue damage in a mouse model of multiple sclerosis. *FASEB J* 2000; **14**: 691–698.

53 Moore TC, Petro TM. IRF3 and ERK MAP-kinases control nitric oxide production from macrophages in response to poly-I:C. *FEBS Lett* 2013; **587**: 3014–3020.

54 Yang C-S, Kim J-J, Lee SJ, Hwang JH, Lee C-H, Lee M-S *et al.* TLR3-triggered reactive oxygen species contribute to inflammatory responses by activating signal transducer and activator of transcription-1. *J Immunol* 2013; **190**: 6368–6377.

55 Zhang W, Kuncewicz T, Yu ZY, Zou L, Xu X, Kone BC. Protein-protein interactions involving inducible nitric oxide synthase. *Acta Physiol Scand* 2003; **179**: 137–142.

56 Junttila MR, de Sauvage FJ. Influence of tumour micro-environment heterogeneity on therapeutic response. *Nature* 2013; **501**: 346–354.

57 Oshiumi H, Okamoto M, Fujii K, Kawanishi T, Matsumoto M, Koike S *et al.* The TLR3/TICAM-1 pathway is mandatory for innate immune responses to poliovirus infection. *J Immunol* 2011; **187**: 5320–5327.

58 Tanaka H, Mori Y, Ishii H, Akedo H. Enhancement of metastatic capacity of fibroblast-tumor cell interaction in mice. *Cancer Res* 1988; **48**: 1456–1459.

Figure legends

Figure 1. TICAM-1-dependent inhibition of tumor growth and caspase-8/3 activation in tumors

(a) Tumor growth in B6 WT, TICAM-1$^{-/-}$, or MAVS$^{-/-}$ mice. PBS or polyI:C (100 μg) was injected s.c. as indicated by the arrows. (b) Tumor growth in B6 WT mice treated with anti-CD8β, anti-NK1.1, or anti-CD4 Abs. PBS/polyI:C or Ab was injected as indicated by the arrows or arrow heads, respectively. The results represent the mean ± standard deviation (SD) (n = 3–5, $^{**}P < 0.005$, n.s., not significant) (a, b). (c) TUNEL staining in tumors at 24 h after PBS or polyI:C (200 μg) injection (i.p.). (d) Caspase-3 activation in tumors implanted in WT, TICAM-1$^{-/-}$, MAVS$^{-/-}$, or IFNAR1$^{-/-}$ mice at 18 h after polyI:C injection. Scale bars: 200 μm. (e, f) Western blot analysis of tumors isolated from mice at 18 h (e) or 7 h (f) after PBS or polyI:C (200 μg) injection. The intensity of the bands indicated by asterisks was quantified using ImageJ software and normalized to GAPDH. All data are representative of at least two independent experiments.

Figure 2. CD11b^{+}Ly6G^{+} cells are essential and sufficient for the TICAM-1-induced anti-tumor effect

(a) Tumor growth of EL4 cells in an anti-Gr1 Ab-treated B6 WT mice. Abs were injected i.p. on day 7 and 11. PBS or polyI:C (100 μg) was injected s.c. on day 8 and 12. (b) Tumor growth in isotype control Ab or anti-Ly6G Ab-treated B6 WT mice. Abs were injected i.p. on day 9 and 13. PBS or polyI:C (100 μg) was injected s.c. on day 10 and 14. The results represent the mean ± standard deviation (SD) (n = 3–4, $^{*}P<0.05$, n.s., not significant). (c) Western blot analysis of tumors isolated from Ly6G^{+} cell-depleted mice 18 h after injection of PBS or polyI:C (200 μg). (d) CD11b^{+}Ly6G^{+} cells (1 x 10^{6}) isolated from PBS or polyI:C-treated B6 WT or TICAM-1$^{-/-}$ tumor-bearing mice were mixed with EL4 cells (5 x 10^{5}), and the mixture was injected s.c. into B6 WT mice on day 0 (n = 4, $^{*}P<0.05$). (e) Cytotoxic activity of CD11b^{+}Ly6G^{+} cells isolated from the spleen of tumor-bearing WT or TICAM-1$^{-/-}$ mice, 4 h after treatment with polyI:C (200 μg).

Data represent mean ± SD. (n = 3, $**P < 0.005$) Data are representative of at least two independent experiments.

Figure 3. Sensitivity of EL4 cells to PNT or H_2O_2

(a, b, d, and e) EL4 cells (1×10^4) were cultured in the presence of PNT (a and b) or H_2O_2 (d and e). After 24 h, cell viability was determined by a WST-1 assay (a and d), or after 8 h, caspase-8/3 activation was analyzed by immunoblotting (b and e). (c) EL4 cells (2×10^5) were pre-treated with uric acid (2 mg/mL) for 1 h, and then cultured in the presence of PNT for 24 h. Cells were analyzed by flow cytometry. Dead cells were determined by 7-AAD staining. Data are shown as mean ± standard deviation (SD). (n = 3) Representative data of two independent experiments are shown.

Figure 4. ROS/RNS production by $CD11b^+Ly6G^+$ cells in tumor-bearing mice

(a-d) EL4 tumor-bearing mice were injected i.p. with PBS or polyI:C (200 μg). (a) After 8 h, the tumor cell suspension was analyzed by flow cytometry using an anti-iNOS Ab. (b) After 3 h, $CD11b^+Ly6G^+$ cells were isolated from the spleen of tumor-bearing mice. iNOS and NOX2 mRNA expression in B6 WT or TICAM-$1^{-/-}$ $CD11b^+Ly6G^+$ cells was determined by quantitative RT-PCR analysis. (n = 3, $*P<0.05$.) (c) The tumor cell suspension was stained with APF and anti-Ly6G Ab and analyzed by flow cytometry. (d) After 5 h, mice were injected i.p. with PBS or L-NAME (1.5 mg). The tumor cell suspension was analyzed by flow cytometry 2 h later. (e-g) EL4 tumor-bearing B6 WT (e, f, and g), TICAM-$1^{-/-}$ (e and f), or IFNAR$1^{-/-}$ (g) mice were injected with PBS or polyI:C (200 μg). After 7 h, the tumor cell suspension was stained with APF or HPF and analyzed by flow cytometry. Graph represents the average of APF-stained $Ly6G^+$ cells in the tumor cell suspension (n = 3, $**P<0.005$) (e). (h) EL4 tumor-bearing mice were injected with PBS or

polyI:C. After 8 h, the tumor cell suspension was analyzed by flow cytometry using a BES-H_2O_2 reagent. All data are representative of at least two independent experiments.

Figure 5. PolyI:C-activated $CD11b^+Ly6G^+$ cells inhibit tumor growth through ROS/RNS production

(a and b) $CD11b^+Ly6G^+$ cells were isolated from tumor-bearing mice after a 4 h treatment with PBS or polyI:C (200 μg), and then mixed with EL4 cells. The mixture was injected s.c. into B6 WT mice, followed by an i.p. injection with 20 mg of uric acid (a) or 1.5 mg of L-NAME (b) (day 0). (c) EL4 tumor-bearing mice were injected i.p. with PBS or polyI:C (200 μg). After 4 h, $CD11b^+Ly6G^+$ cells were isolated from spleens in the presence or absence of 50 μM L-NIL. The cytotoxic activity of $CD11b^+Ly6G^+$ cells against EL4 cells was determined. Data are shown as mean ± standard deviation (SD). (n = 3, **P<0.005.) Representative data of two independent experiments are shown.

Figure 6. Cancer cell lines are sensitive to ROS/RNS-induced cell death

(a) Tumor growth of B16 cells in an anti-Ly6G Ab-treated B6 WT mice. Abs were injected i.p. on day 12 and 16. PBS or polyI:C (100 μg) was injected s.c. on day 13 and 17. (b) $CD11b^+Ly6G^+$ cells (1×10^6) isolated from PBS or polyI:C-treated B6 WT mice bearing B16 tumor were mixed with B16 cells (3×10^5), and the mixture was injected s.c. into B6 WT mice on day 0 (n = 3-4, *P<0.05). (c) B16 tumor-bearing mice were injected i.p. with PBS or polyI:C (200 μg). After 7 h, a single cell suspension of tumor or spleen was stained with APF or HPF, and analyzed by flow cytometry. (d-f) EL4 cells (1×10^4), 3LL cells (1×10^4), B16 cells (0.25×10^4), and MC38 cells (1×10^4) were cultured for 24 h in the presence of PNT (d) or H_2O_2 (e). Cell viability was determined by the WST-1 assay. (f) Cleaved caspase-8 or cleaved caspase-3 was detected by immunoblotting after PNT treatment for 8 h. Data are representative of two independent experiments.

Figure 7. EL4 cells enhance PNT production by $CD11b^{+}Ly6G^{+}$ cells

(a) $CD11b^{+}Ly6G^{+}$ cells isolated from EL4 tumor-bearing mice were activated with PBS or polyI:C (100 μg/mL) in the presence or absence of EL4 cells or recombinant GM-CSF (10 ng/mL). After 7 h, $CD11b^{+}Ly6G^{+}$ cells were stained with HPF and analyzed by flow cytometry. (b) $CD11b^{+}Ly6G^{+}$ cells were cultured with EL4 cells. Cells were separated by insertion of a transwell (0.4 μm-pore size) and activated with polyI:C as in (a). Graphs show the percentage of ROS/RNS-producing cells in total $Ly6G^{+}$ cells. Data are representative of two independent experiments.

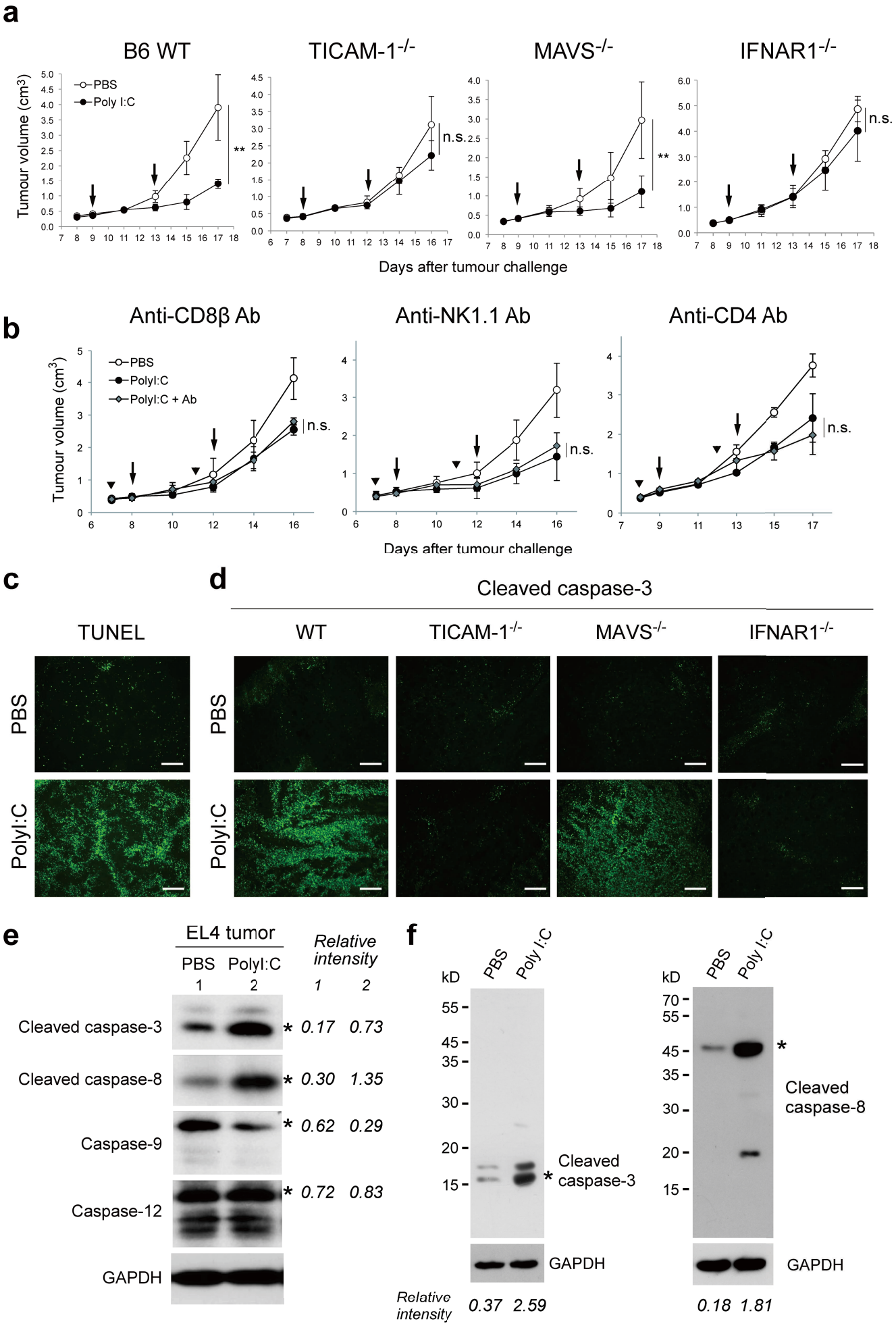

Figure 1 Shime et al.

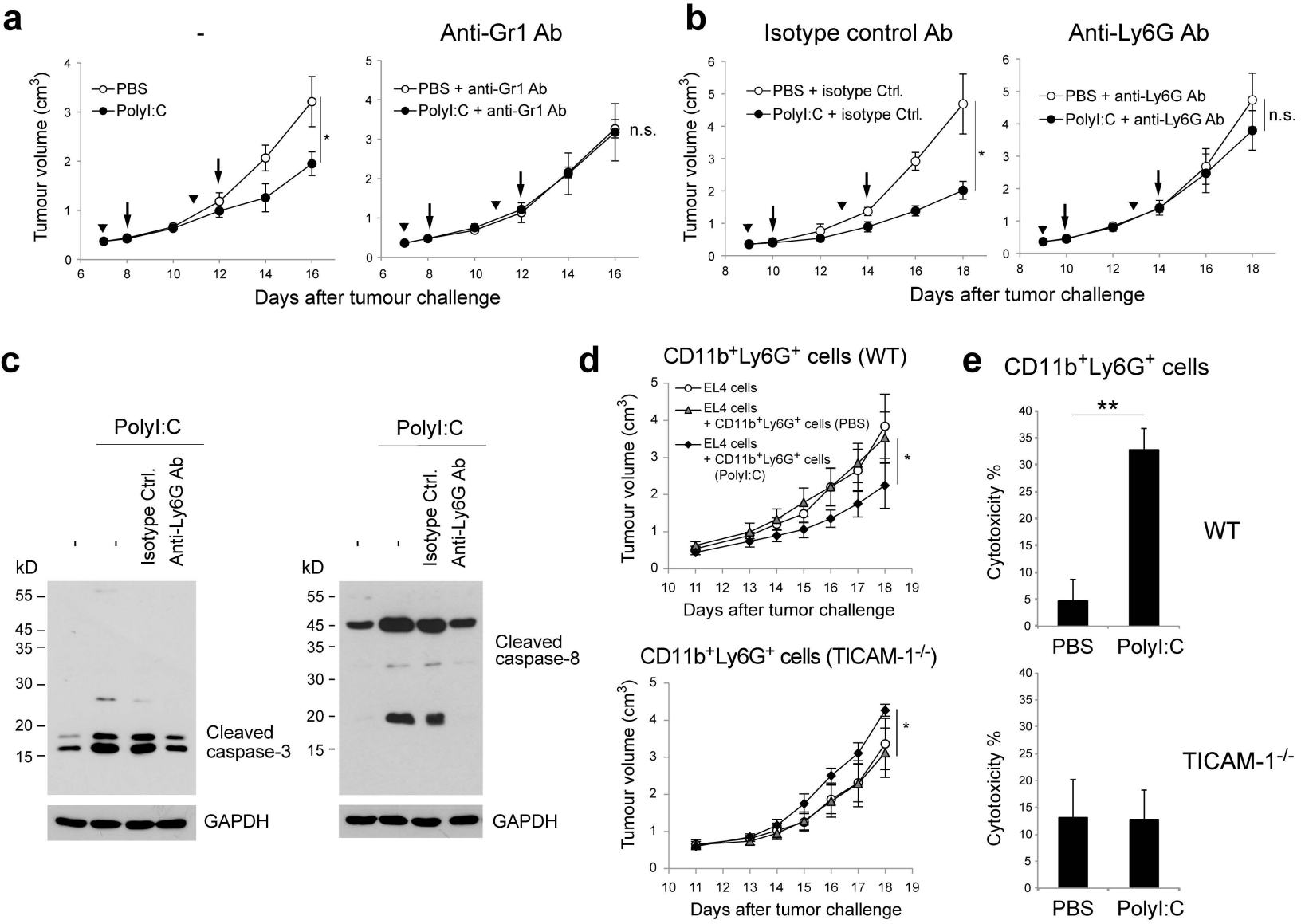

Figure 2 Shime et al.

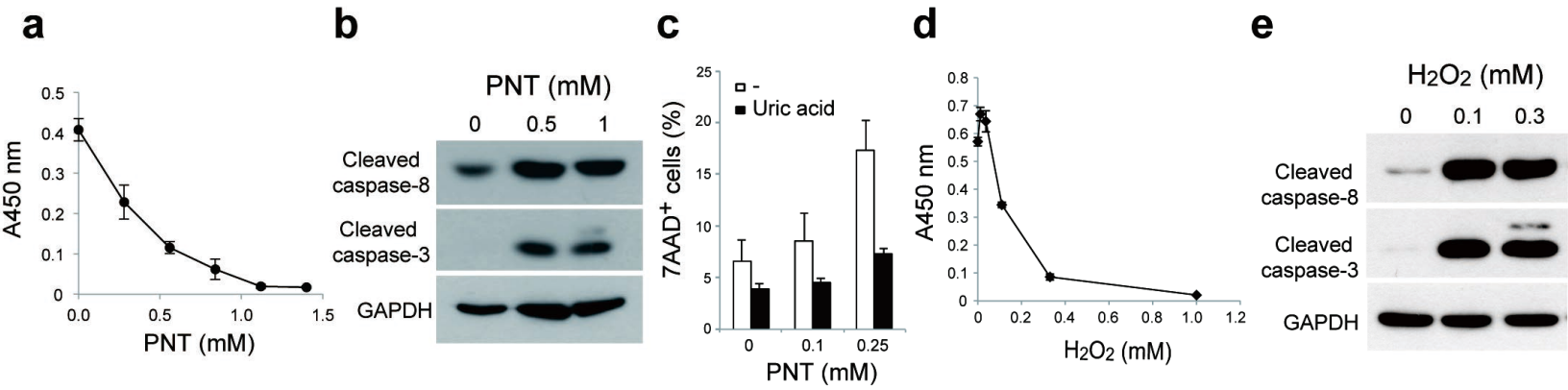

Figure 3 Shime et al.

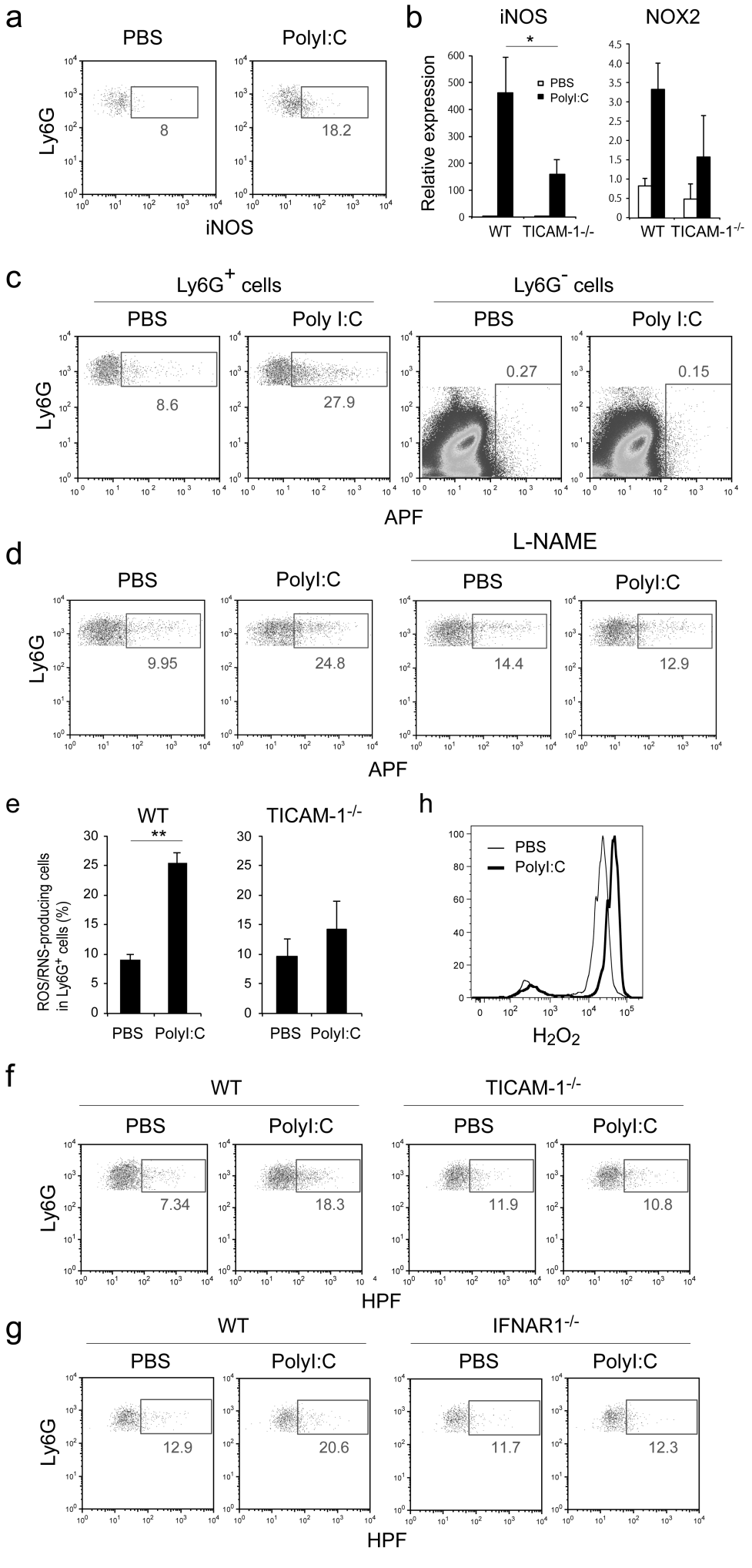

Figure 4 Shime et al.

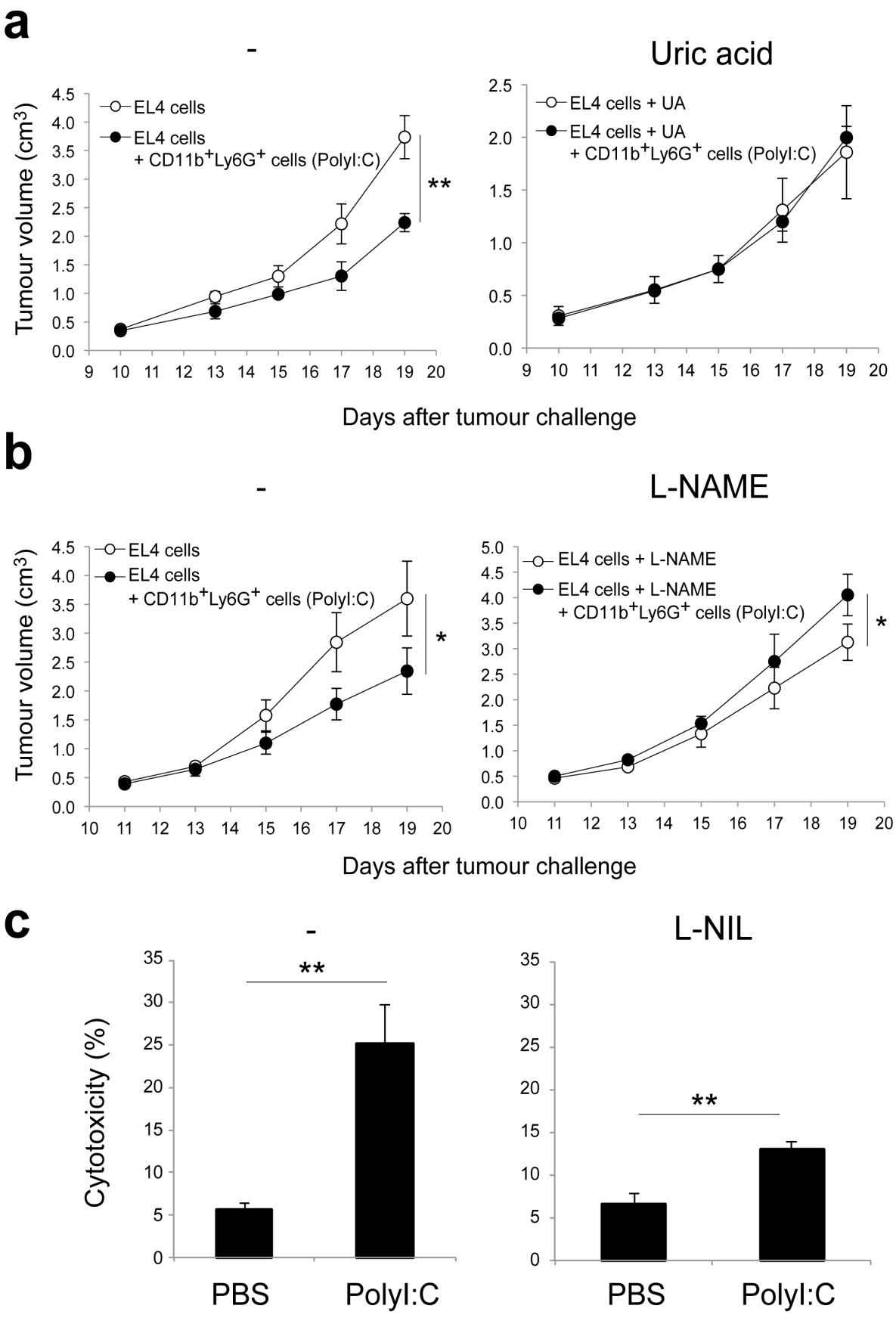

Figure 5 Shime et al.

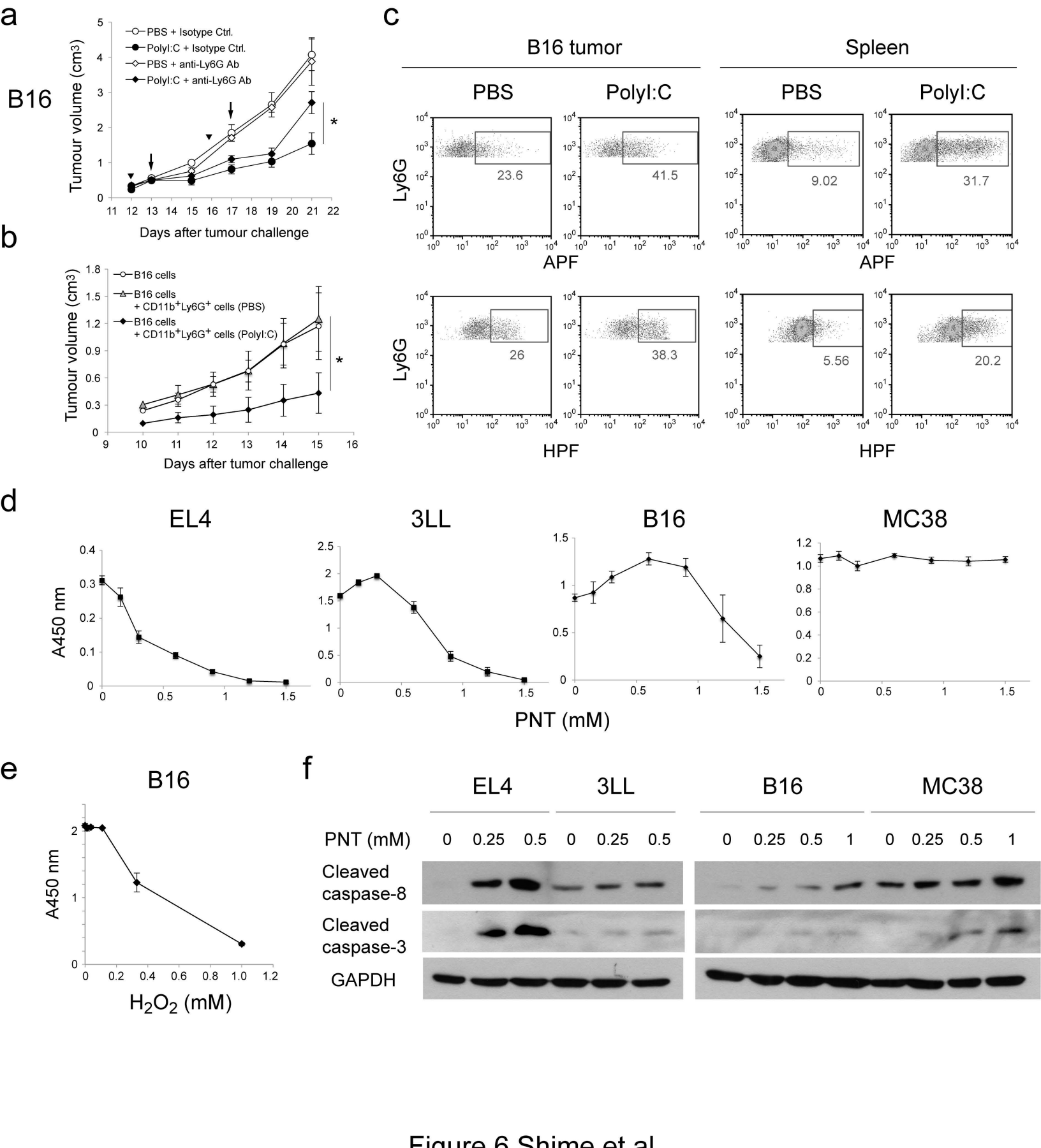

Figure 6 Shime et al.

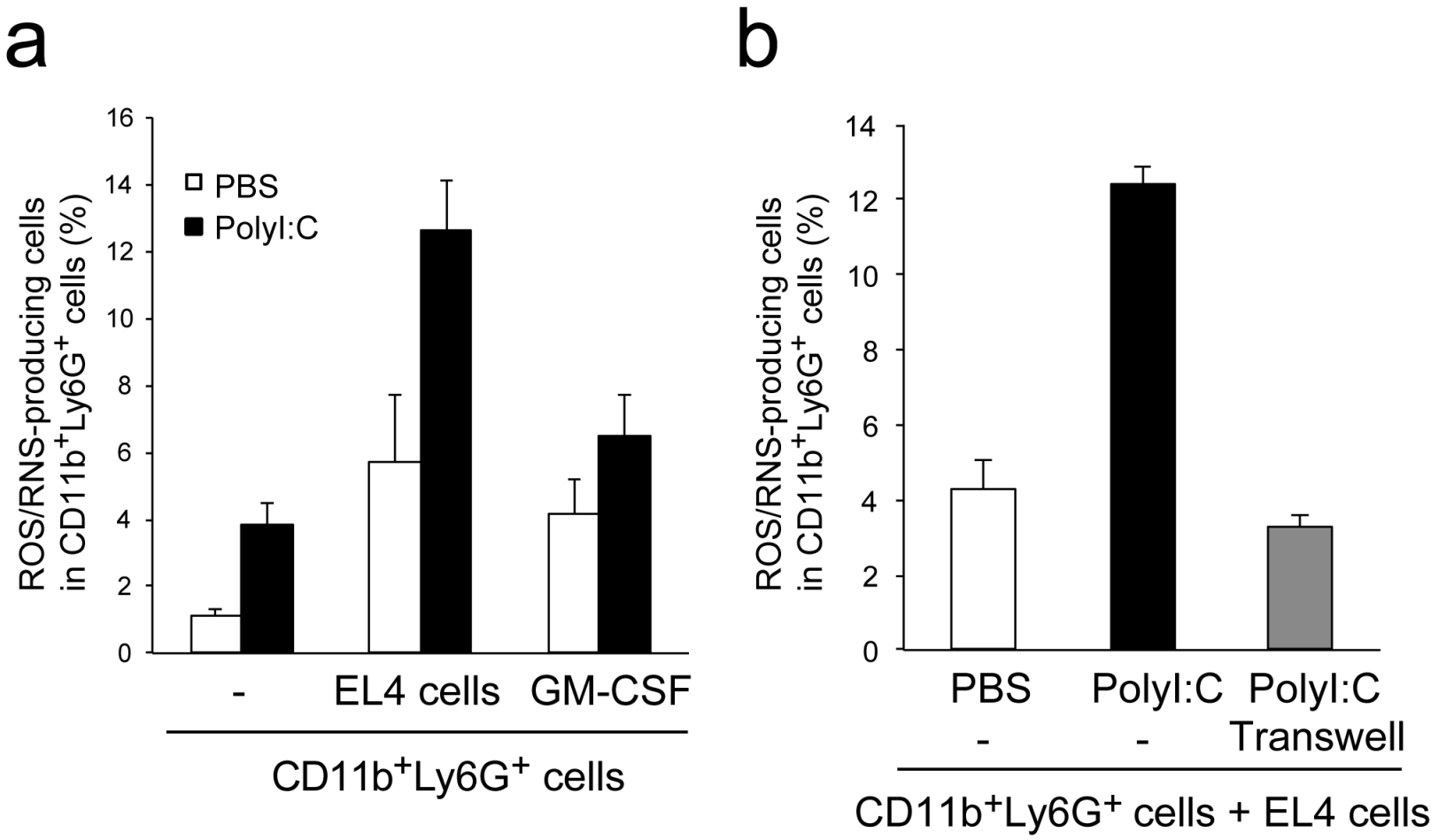

Figure 7 Shime et al.